Optical and Quantum Electronics (2022) 54:354
https://doi.org/10.1007/s11082-022-03674-z

Structural and optical characterization of titanium–carbide and polymethyl methacrylate based nanocomposite

Jelena Pešić[1] · Andrijana Šolajić[1] · Jelena Mitrić[1] · Martina Gilić[1] · Ivan Pešić[2] · Novica Paunović[1] · Nebojša Romčević[1]

Received: 11 October 2021 / Accepted: 10 March 2022 / Published online: 12 May 2022

Abstract

The rich chemistries and unique morphologies of titanium carbide MXenes, made them strong candidates for many applications like sensors and electronic device materials. During the synthesis procedure, chemical etching, oxidation occurs and residual materials, like titanium-dioxide nanocrystals and nanosheets are often present in resulting material. As titanium-carbide MXenes are suggested to be used as additive in organic polymer matrices for production of nanocomposites, it is essential to consider the presence of the oxides and other residuals together with MXene flakes in synthesis results, and consequently in produced nanocomposite. In this study we present structural and optical characterization of such polymer nanocomposite titanium carbide/PMMA (Polymethyl methacrylate) consisting of Ti_3C_2, TiC_2 MXenes and TiC, and TiO_2 residues of synthesis in PMMA matrix, as a multicomponent nanocomposite. Using XRD, infra-red and Raman spectroscopy, followed by comparative study on the vibrational properties using density functional theory calculations, we characterize this nanocomposite. Further, the SEM measurements are performed, demonstrating the produced titanium-carbide-based flakes in nanocomposite are well defined and separated to nanosized grains, allowing us to use Maxwell–Garnet model to analyse infrared spectrum. This enables us to determine the presence of the optical modification of polymer matrices corresponding to a volume fraction of 0.25.

Keywords Titanium-carbide nanoparticles · PMMA composite · Multicomponent nanocompostite

This article is part of the Topical Collection on Photonics:Current Challenges and Emerging Applications.

Guest edited byJelena Radovanovic, Dragan Indjin, Maja Nesic, Nikola Vukovic andMilena Milosevic.

✉ Jelena Pešić
yelena@ipb.ac.rs

[1] Institute of Physics Belgrade, University of Belgrade, Pregrevica 118, Belgrade 11080, Serbia

[2] Faculty of Technology and Metallurgy, University of Belgrade, Belgrade 11000, Serbia

1 Introduction

Nanocomposites are the combination of two or more different materials where a minimum of one of the components has dimension less than 100 nm Twardowski (2007). The polymer nanocomposites are made of organic polymer matrix (in this research, polymethyl methacrylate—PMMA) and inorganic components (titanium carbide nanoparticles). The properties of the obtained nanocomposites depend on the individual properties of each component, morphology and the interface characteristics. In an attempt to improve the properties of conventional polymer materials and extend the fields of their applications, functionalization has emerged as important method in improvement of their not satisfactory electronic, thermal and mechanical properties Tamborra et al. (2004); Hussain et al. (2006). In addition to typical advantages of polymers (such are light-weight, low cost, and good processability), the improvement of electrical properties (e.g., electrical conductivity) with the addition of a small amount of conductive fillers into polymer matrices have promoted polymer nanocomposites into versatile multifunctional materials. Many applications like household electronics, memory and microwave devices are potentially available with addition of metal oxide nanoparticles to polymer. This enables the modification of the polymer's physical properties as well as the implementation of new features in the polymer matrix creating new type of materials known as the polymer nanocomposites. PMMA as a thermoplastic polymer, has many extraordinary properties, like great transparency and ultraviolet resistance, high abrasion resistance, hardness and stiffness and making it widely used in many applications ranging from everyday items to high tech devices. Further, PMMA is nondegradable and biocompatible which makes it an excellent candidate in medical applications like tissue engineering with typical applications such as fracture fixation, intraocular lenses and dentures Peppas and Langer (1994).

Multicomponent nanocomposites based of layered and 2D materials have drawn significant attention in past decade with promises of various applications. Reduction of dimensionality of the system to the truly atomic-scale 2D is related to the occurrence of all new amazing properties in low-dimensional material, since the reduction of available phase space and decreased screening lead to enhancement of quantum effects and increased correlations. Low-dimensional materials have been studied intensively both for their fundamental properties and insight in basic principles of matter but as well for their colossal potential for applications. A discovery of true two-dimensional material graphene Novoselov et al. (2004) and its remarkable properties like and experimental observation of Klein tunnelling, quantum Hall effect and superconductivity Novoselov et al. (2004); Katsnelson et al. (2006); Zhang et al. (2005); Durajski et al. (2019); Pešić et al. (2014); Margine et al. (2016); Durajski et al. (2020) paved the way for investigation of a new family of materials in low-dimensional physics. The new field of two-dimensional materials research has arose and investigated not only graphene but many more crystal structures where, just like in graphene, cells are connected in at least one direction by the van der Waals' forces Novoselov et al. (2016).

Transition metal carbides are important group of materials for applications since they possess some desired characteristics such as thermal stability, wear and corrosion resistance, electronic, magnetic as well as catalytic properties. Titanium-carbide powders are generally used for manufacturing cutting tools, used in treatment of metals and as abrasive-resistant materials. In 2011 Naguib et al. (2011), the group of early transition metal carbides and/or carbo-nitrides labeled as MXenes. MXenes are produced by the etching out of the A layers from MAX phases Naguib et al. (2011, 2012, 2013). Name MAX phase comes from its chemical composition: $M_{n+1}AX_n$, where M is an early transition metal, A is mainly a group IIIA or IVA (i.e., groups 13 or 14) element, X is carbon and/or nitrogen, and n = 1, 2, or 3.

During the synthesis of titanium-carbide MXenes by chemical etching, oxidation can occur which results in presence of TiO_2 consisted of nanosheets and numerous TiO_2 nanocrystals Naguib et al. (2014). There are several studies Zhu et al. (2016); Gao et al. (2015) whose researched is focused in possible applications of TiO_2-MXene structures. It is demonstrated the joint effects of Ti_3C_2 and TiO_2 endowed TiO_2-Ti_3C_2 nanocomposites with excellent properties and improved functionalities Zhu et al. (2016). In this work we investigate the structural and optical properties of polymer nanocomposites prepared by the incorporation of titanium-carbide nanoparticles consisting of Ti_3C_2, TiC_2 TiC and TiO_2 into the matrices of polymer PMMA. The sample of nanocomposite material was prepared, the PMMA matrix with titanium-carbide particles, PMMA/TiC. As for similar materials Shan et al. (2021, 2020, 2021); Tan et al. (2021); Jafari et al. (2020); Tan et al. (2021) proper understanding of composition of materials used in composite is crucial and XRD analysis for the titanium-carbide flakes. The structural and morphology studies of the nanocomposites were carried out by SEM and Raman spectroscopy. Infrared spectroscopy is a very powerful technique in analysis of various nanoparticle and nanocomposite materials prepared in various techiques Dastan (2015); Dastan and Chaure (2014); Dastan et al. (2014); Dastan and Chaure (2017). To further understand properties of our inhomogenious nanocomposite we used infrared spectroscopy with Maxwell–Garnet model. To further support optical characterization, calculations based on density functional theory were performed.

2 Samples preparation and structural characterization

2.1 Titan-carbide/PMMA composite synthesis

In this work, titanium-carbide/PMMA nanocomposite sample was made from mixture of MXene based titanium-carbide nanoflakes in PMMA matrix. Production of layered titan-carbide flakes is based on MXene synthesis by selective etching of Al atomic layers from Ti_3AlC_2 MAX phase, we used the so-called 'mild' method with lithium fluoride (LiF) and hydrochloric acid (HCl) Tu et al. (2018). This method was described in Naguib et al. (2011). Procedure of composite preparation is described in Fig. 1.

Commercially available PMMA Acryrex CM205 (Chi Mei Corp. Korea, (Mw ≈ 90400 g/mol, $n = 1.49$, $\lambda = 633$ nm) pellets were used as a matrix for sample preparation. Ti_3AlC_2 MAX phase was processed and kindly donated from Layered Solids Group, Drexel University. Titanium-carbide flakes were obtained by sonification in the water and drying the supernatant in a Petri dish in the oven for 30 minutes on 90◦C.

Composite was prepared with 10 wt% PMMA solution in acetone (Carlo Erbe Reagents, Spain) and added dried titanium-carbide flakes. After stirring the solution was poured in Petri dish Cao et al. (2017) and dried in oven 24h on 40 °C. Content of titanium-carbide flakes in the sample was 1.7 wt%.

The morphology of the produced composite has been investigated by FESEM using high resolution electron microscope MIRA3 TESCAN. Samples display separated nano-sized grains. Fig. 2a presents FESEM image of MXene flakes delaminated in water showing morphology of obtained flakes, b FESEM image of the PMMA/titanium-carbide

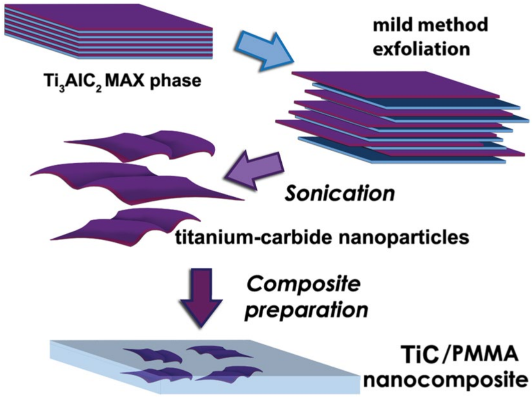

Fig. 1 Schematic describing the synthesis process of MXenes from MAX phases and preparation of composite

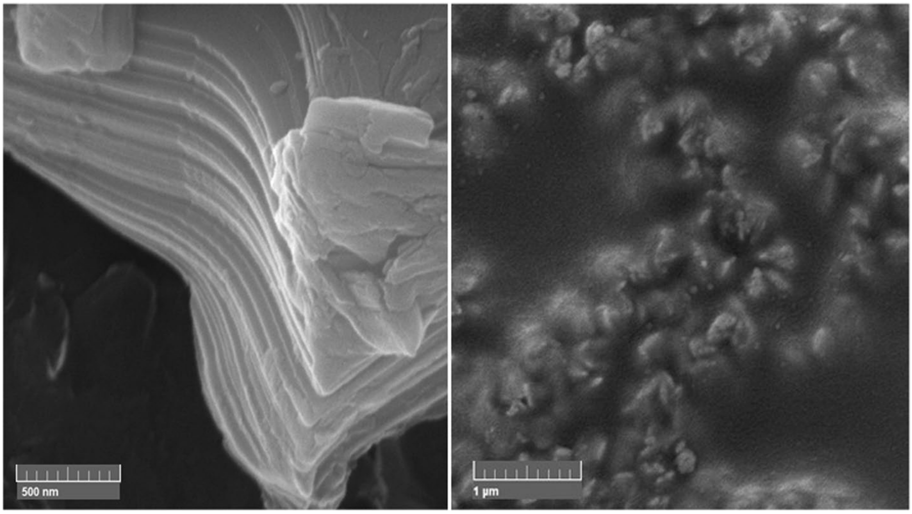

Fig. 2 FESEM photos of **a** Flakes delaminated in water; **b** PMMA composite prepared with titanium-carbide flakes

nanocomposite. Characteristic layered structure of MXenes is visible on FESEM image and confirming success of delamination and exfoliation procedures. Obtained flakes demonstrate multilayered structure with few μm in diameter. In Fig. 2b typical accordion like structure can be indicated in nanosize grain-like structures, clustered in PMMA matrix.

2.2 XRD

X–ray diffraction powder (XRD) technique was used to determine structural characteristics of titanium-carbide based flakes to be used in composites. Philips PW 1050 diffractometer equipped with a PW 1730 generator was used. The same conditions were used for all samples, 40 kV×20 mA, using Ni filtered Co Kα radiation of 0.1778897 nm at room temperature. Measurements were carried out in the 2θ range of 20–80° with a scanning step

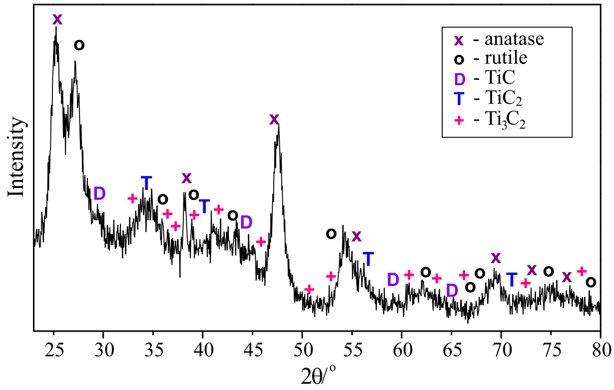

Fig. 3 XRD pattern for titanium-carbide flakes, starting material for PMMA/TiC composite

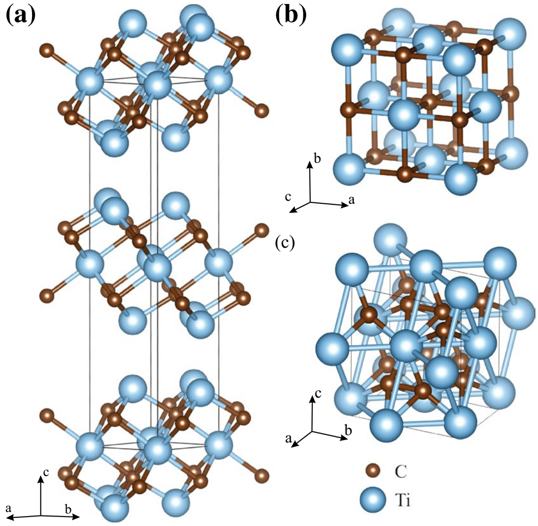

Fig. 4 Schematic representation of Titanum-carbide structures present at composite **a** Ti_3C_2, **b** TiC and **c** TiC_2

of 0.05° and 10 s scanning time per step. In Fig. 3 is presented XRD pattern for titanium-carbide flakes, starting material for composite. The different phases of titanium carbide can be noticed from diffractogram—Ti_3C_2, TiC and TiC_2 together with TiO_2. TiO_2 is widely present as anatase and rutile. All peaks obtained correspond to the structures of Ti_3C_2, TiC, TiC_2, anatase and rutile and it is confirmed that they belong to space groups $P6_3/mmc$ (194), $Fm3\overline{m}$ (225) Fm2m (42), $I4_1/amd$ (141), $P4_2/mnm$ (136), respectively. The unit cells of MXene structures Ti_3C_2, TiC and TiC_2 are presented in Fig. 4. These structures were further used in DFT analysis of optical spectroscopy results in Sect. 3.3.

3 Results and discussion

3.1 Raman spectroscopy

The micro-Raman spectra were taken in the backscattering configuration and analyzed by the TriVista 557 system equipped with a nitrogen cooled charge-coupled-device detector. As an excitation source, we used the 532 nm line of Ti:Sapphire laser. Excitation energy is in the off-resonance regime for all the considered materials. The Raman spectra of the PMMA, PMMA/TiC, and titanium-carbide flakes, measured in the spectral range of 100-1100 cm^{-1} at room temperature, are presented in Fig. 5.

The Raman spectrum of PMMA is presented in Fig. 5a. Intense modes at 235, 300, 362, 400, 484, 560, 603, 660, 733, 815, 839, 864, 911, 967, 985, 1063 and 1091 cm^{-1} were detected. The obtained results are in a good agreement with the values given in the literature Willis et al. (1969); Thomas et al. (2008); Ćurčić et al. (2020).

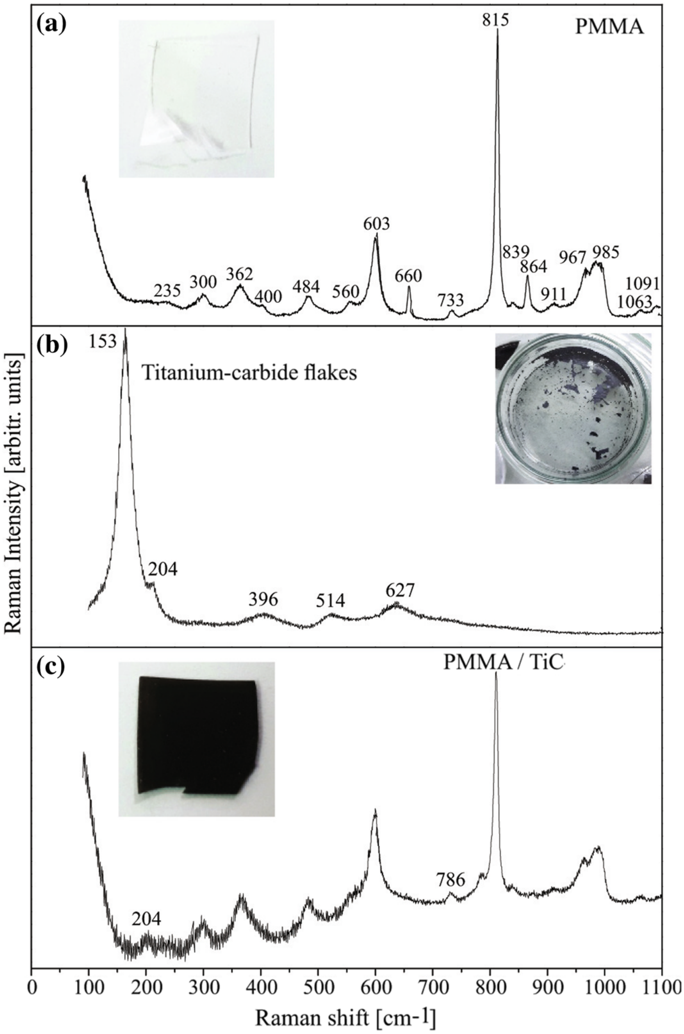

Fig. 5 Raman spectra with photo of the sample of **a** PMMA, **b** Titanium-carbide flakes, **c** PMMA/TiC composite. Only titanium-carbide related peaks are marked in this spectrum. Unassigned peaks correspond to PMMA from **a** spectrum

In Fig. 5b spectrum of titanium-carbide flakes after etching procedure is presented. Several characteristic peaks can be distinguished on 153 cm^{-1}, 204 cm^{-1}, 396 cm^{-1}, 514 cm^{-1} and 627 cm^{-1}. Peaks at 153 cm^{-1} and 627 cm^{-1} correspond to doubly degenerated E_{2g} modes of Ti_3C_2. The frequency associated with E_{2g} modes is calculated to be at 161 cm^{-1} for the bare Ti_3C_2. Since their main contribution is from in-plane vibrations of Ti and C atoms, it can be influenced by the vibrations of the terminal atoms (as a residue of synthesis procedure) weaken the in-plane motion of the Ti and C atoms, hence there is shift to lower frequency. The terminal groups play significant roles for the vibrational modes: the terminal atoms weakening the motions in which the surface Ti atoms are involved while strengthening the out-of-plane vibration of the C atoms; the corresponding vibrational frequencies dramatically change with the various terminal atoms Zhao et al. (2016). This is consistent with XRD results suggesting significant amount of TiO_2 as a residue of synthesis procedure as described in introduction. This can be also visible in Raman spectrum of titanium-carbide flakes on 204 cm^{-1} and 514 cm^{-1}. The doubly degenerated modes at 621 cm^{-1} correspond to the in-plane vibration of the C atoms Hu et al. (2015). In Fig. 5c spectrum of PMMA/TiC is presented, only titanium-carbide related peaks at 204 and 786 cm^{-1} are marked in this spectrum. Unassigned peaks correspond to PMMA peaks marked on a) panel.

As XRD analysis demonstrated, obtained flakes contain both MXene flakes and titanium-dioxide as the residue of synthesis procedure. To further understand and assign this spectra we performed theoretical analysis of all materials identified in XRD pattern using density functional theory calculations. Calculations provided us a guide for identification of peaks and all results are summarized in Table 1.

3.2 Far-infrared spectroscopy

Far-infrared reflection spectra were measured at room temperature in the spectral range from 40 to 600 cm^{-1}, carried out with a BOMEM DA 8 spectrometer. The experimental data are represented at Fig. 6a and by circles at Fig. 6b–d. As expected, the reflection spectra of nanocomposites are by intensity placed between the starting composites. In order to analyse far-infrared spectra we have used the classical oscillator model with free carrier contribution, as a base for Maxwell–Garnet effective medium approximation Abstreiter (1984); Carter and Bate (1971). The low-frequency dielectric properties of single crystals are described by classical oscillators corresponding to the TO modes, to which the Drude part is superimposed to take into account the free carrier contribution:

$$\epsilon_s(\omega) = \epsilon_\infty + \sum_{k=1}^{l} \frac{\epsilon_\infty S_k}{\omega_{TOk}^2 - \omega^2 - i\gamma_{TOk}\omega} - \frac{\epsilon_\infty \omega_P^2}{\omega(\omega + i\Gamma_P)}, \quad (1)$$

where ϵ_∞ is the bound charge contribution and it is assumed to be a constant, ω_{TOk}^2 is the transverse optical-phonon frequency, ω_P^2 the plasma frequency, γ_{TOk} is damping, Γ_P is the plasmon mode damping coefficient, and S_k is the oscillator strength.

In general, the optical properties of an inhomogeneous material are described by the complex dielectric function that depends on 3D distribution of constituents. The investigated mixture consists of two materials with two different dielectric components. One is treated as a host, and the other as the inclusions. The characterization of the inhomogeneous material by the two dielectric functions is not useful, since one need to know the exact geometrical arrangement of the constituents of the material. However, if the wavelength of

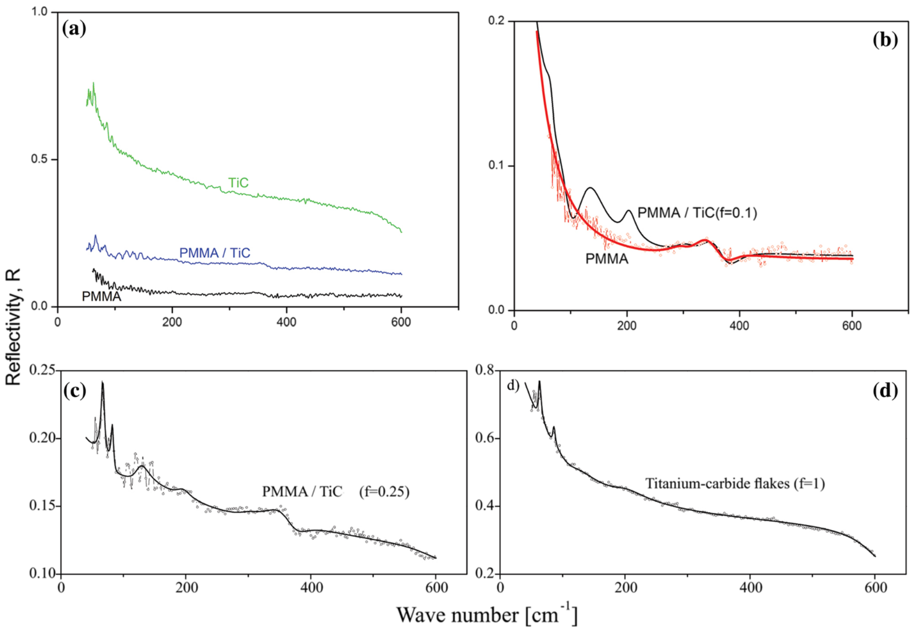

Fig. 6 Infrared analysis: **a** Infrared spectra of Titanium-carbide flakes (green) and composites PMMA/TiC (blue) and pure PMMA (black), **b**, **c**, and **d** circles represent experimental data and solid lines are fit obtained by Maxwell–Garnet model as described in Sect. 3.2

Table 1 Raman and infrared spectrum analysis and modes assignation for synthesized titanium-carbide flakes and PMMA/TiC composite

	Titanium-carbide flakes		PMMA/TiC		Description
	Raman	IR	Raman	IR	
ω_1		62.4		66	E_u, Ti_3C_2
ω_2		85.8		81	B_1, TiO_2 rutile
ω_3		119		127	A_{2u}, Ti_3C_2 and B_1 TiC_2
ω_4	153				E_g, Ti_3C_2
ω_5	204	200	204	195	E, TiO_2 anatase
ω_6	396				A_2, TiC_2; E, TiO_2 anatase
ω_7	514				A_1, TiO_2 anatase
ω_8		620		615	E_u, Ti_3C_2
ω_9	627				E_g, Ti_3C_2
ω_{10}			786		A_g, TiO_2 rutile
ω_P		80		150	
f		1		0.25	

Infrared modes fit is obtained by Maxwell–Garnet model. Modes assignation is performed using values obtained in DFT calculations

the electromagnetic radiation is much larger than the size of inclusions, classical theories of inhomogeneous material presume that the material can be treated as a homogeneous substance with an effective dielectric function. In the literature, many mixing models can be found for the effective permittivity of such mixture. Some are present in ref Sihvola (1999). Optical properties of such materials depend upon the properties of constituents, as well as their volume fraction. Since our samples are well defined and separated nanosized grains (as demonstrated on FESEM images, Fig. 2), we used Maxwell–Garnet model for present case. For the spherical inclusions case, the prediction of the effective permittivity of mixture, ϵ_{eff}, according to the Maxwell–Garnet mixing rule is Garnett (1904):

$$\epsilon_{eff} = \epsilon_1 + 3f\epsilon_1 \frac{\epsilon_2 - \epsilon_1}{\epsilon_2 + 2\epsilon_1 - f(\epsilon_2 - \epsilon_1)} \tag{2}$$

Here, spheres of permittivity ϵ_2 (Titanium-carbide) are located randomly in homogeneous environment ϵ_1 (PMMA) and occupy a volume fraction f.

Solid lines in Fig. 6 are calculated spectra obtained by a fitting procedure based on the previously presented model. The agreement of the theoretical model obtained in this manner with the experimental results is excellent.

To demonstrate the model, together with the infrared spectrum of PMMA, Fig. 6b is given the theoretical spectrum of PMMA/TiC nanocomposites for f = 0.1. The properties of TiC structures are clearly visible. A larger share of TiC structures leads to the spectrum in Fig 6c, which was obtained for f = 0.25. In Fig. 6d, for f=1 of course there is no effect from PMMA.

3.3 Discussion

In Table 1 are summarized results from spectroscopic measurements of obtained nanocomposites. As stated above, for infrared measurements the agreement of the theoretical model with obtained spectra is excellent and best fit parameters are presented in this table.

To further support our results we performed DFT based calculations and calculated vibrational frequencies in Γ point for all materials present after titanium-carbide flakes exfoliation, which we determined are present using XRD, Fig. 3. Obtained values are compared to experimental Raman and infrared spectrum and modes have been assigned. Results are summarized in Table 1. We presented only modes that can be assigned to peaks from the spectra. In infrared spectra we can notice good agrement with theoretical calculations, specially for low-energy E_u and A_{2u} mode of Ti_3C_2 which is present the composite spectrum (Fig. 6b, c) as in starting titanium-carbide material (Fig. 6d). As shown in XRD we notice peaks originating from TiO_2 and TiC_2 in mid-energy region. High-energy mode E_u on 620 cm^{-1} is present in spectrum of PMMA/TiC. In Table 2 are summarized calculated optical modes for Ti_3C_2 with symmetry 194 group used in analysis.

DFT calculations were performed using the Quantum Espresso software package Giannozzi (2009), based on the plane waves and pseudopotentials. The PBE (Perdew, Burke and Ernzehof) Perdew et al. (1996) exchange-correlation functional was employed and PAW (Projector augmented waves) pseudopotentials were used. Energy cutoff for wavefunctions and charge density were set to 52 Ry and 575 Ry to ensure the convergence. The Brillouin zone was sampled using the Monkhorst-Pack scheme, with 8×8×8 k-points mesh for TiC_2, 8×8×4 for Ti_3C_2, 12×12×12 for TiC, and 8×8×8 for TiO_2 (Rutile and Anatase structures). Phonon frequencies are calculated within the DPFT (Density Functional Perturbation Theory) implemented in Quantum Espresso Baroni et al. (2001). In order to obtain the lattice parameters more accurately, van der Waals forces were treated using the Grimme-D2 correction Grimme (2006)

Table 2 Vibrational modes for Ti_3C_2 with symmetry group 194, calculated from the measured data

Ti_3C_2 ($P6_3/mmc$)		
cm^{-1}	Symmetry	Raman or IR active
65.0	E_u	I
135.2	A_{2u}	I
160.6	E_g	R
161.4	E_g	R
229.9	A_{1g}	R
269.3	A_{1g}	R
271.1	E_u	I
271.7	E_u	I
371.4	A_{2u}	I
382.4	A_{2u}	I
549.1	A_{2u}	I
554.4	A_{2u}	I
611.2	E_g	R
620.4	E_g	R
624.1	E_u	I
626.4	E_u	I
653.2	A_{1g}	R
658.3	A_{1g}	R

Optical spectroscopy results supported with the DFT numerical calculation confirm that produced composites PMMA/TiC show optical modification comparing to pure PMMA. Our X-ray diffraction investigation of synthesized nanomaterials identified presence of Ti_3C_2 and TiC_2 MXenes and residual TiO_2 and TiC from the synthesis procedure, which can be also supported from the optical spectroscopy results.

4 Conclusion

In this paper, we present results of optical and structural investigation of composite based on titanium-carbide nanoflakes (Ti_3C_2, TiC_2 TiC and TiO_2)in PMMA matrix. X-ray diffraction (XRD) investigation of synthesized nanomaterials identified presence of Ti_3C_2 and TiC_2 MXenes and residual TiO_2 and TiC from the synthesis procedure. The optical properties were studied by Raman and infrared spectroscopy at room temperature. The analysis of the Raman spectra was made by the fitting procedure. For analysis of infrared spectra we used Maxwell–Garnet model. In order to identify and assign vibrational modes, vibrational frequencies of all identified materials were calculated using density functional theory, and compared with experimental results. We confirmed optical modification in composite structure compared to pure PMMA. Further analysis that goes beyond the scope of this publication studies mechanical properties of composite materials, confirming improvements compared to pure PMMA. The obtained composite showed enhanced hardness, elastic modulus and tensile strength compared with pure PMMA Pesic et al. (2019).

Acknowledgements The authors acknowledge funding provided by the Institute of Physics Belgrade and Faculty of Technology and Metallurgy, through the grant by the Ministry of Education, Science and Technological Development of the Republic of Serbia. All calculations were performed using computational resources at Johannes Kepler University, Linz, Austria.

Author Contributions Conceptualization, JP and NR; investigation JP, AŠ, JM, MG, IP, NP; validation, JP, NP, NR; formal analysis, JP, AŠ, JM, MG, NP, NR; writing JP and AŠ; writing–review and editing, JP, AŠ, NP, NR; visualization, AŠ; supervision, NR; project administration, NR; funding acquisition, NR. All authors have read and agreed to the published version of the manuscript.

Funding The authors acknowledge funding provided by the Institute of Physics Belgrade and Faculty of Technology and Metallurgy, through the grant by the Ministry of Education, Science and Technological Development of the Republic of Serbia.

Data availability All additional material is available at authors on request.

Code availability Not applicable.

Declarations

Conflict of interest The Authors declare no conflict of interest.

Ethical approval Not applicable.

Informed consent Not applicable.

Consent for publication All authors consent to publication results presented in manuscript.

References

Abstreiter, G.: Light Scattering in Solids IV. Springer, New York (1984)

Baroni, S., de Gironcoli, S., Dal Corso, A., Giannozzi, P.: Phonons and related crystal properties from density-functional perturbation theory. Rev. Mod. Phys. **73**, 515–562 (2001)

Cao, Y., Deng, Q., Liu, Z., Shen, D., Wang, T., Huang, Q., Du, S., Jiang, N., Lin, C.-T., Yu, J.: Enhanced thermal properties of poly (vinylidene fluoride) composites with ultrathin nanosheets of mxene. RSC Adv. **7**(33), 20494–20501 (2017)

Carter, D.L., Bate, R.T.: The Physics of Semimetals and Narrow-gap Semiconductors: Proceedings, vol. 32. Pergamon, Texas, USA (1971)

Ćurčić, M., Hadžić, B., Gilić, M., Radojević, V., Bjelajac, A., Radović, I., Timotijević, D., Romčević, M., Trajić, J., Romcevic, N.: Surface optical phonon (sop) mode in ZnS/poly (methylmethacrylate) nanocomposites. Physica E **115**, 113708 (2020)

Dastan, D.: Nanostructured anatase titania thin films prepared by sol-gel dip coating technique. J. Atom. Mol. Condens. Matter Nano Phys. **2**, 109–114 (2015)

Dastan, D., Chaure, N.B.: Influence of surfactants on TiO_2 nanoparticles grown by sol-gel technique. Int. J. Mater. Mech. Manuf. **2**, 21 (2014)

Dastan, D., Chaure, N.: Kartha: Surfactants assisted solvothermal derived titania nanoparticles: synthesis and simulation. J. Mater. Sci. **28**, 7784–7796 (2017)

Dastan, D., Londhe, P.U., Chaure, N.B.: Characterization of TiO_2 nanoparticles prepared using different surfactants by sol-gel method. J. Mater. Sci. **25**, 3473–3479 (2014)

Durajski, A.P., Skoczylas, K.M., Szczaeniak, R.: Superconductivity in bilayer graphene intercalated with alkali and alkaline earth metals. Phys. Chem. Chem. Phys. **21**, 5925–5931 (2019). https://doi.org/10.1039/C9CP00176J

Durajski, A.P., Auguscik, A.E., Szczeaniak, R.: Tunable electronic and magnetic properties of substitutionally doped graphene. Physica E **119**, 113985 (2020). https://doi.org/10.1016/j.physe.2020.113985

Gao, Y., Wang, L., Zhou, A., Li, Z., Chen, J., Bala, H., Hu, Q., Cao, X.: Hydrothermal synthesis of TiO_2/Ti_3C_2 nanocomposites with enhanced photocatalytic activity. Mater. Lett. **150**, 62–64 (2015)

Garnett, J.M.: XII. Colours in metal glasses and in metallic films. Philosoph. Trans. R. Soc. Lond. Ser. A **203**, 385–420 (1904)

Giannozzi, P., et al.: QUANTUM ESPRESSO: a modular and open-source software project for quantum simulations of materials. J. Phys. Condens. Matter **21**(39), 395502 (2009)

Grimme, S.: Semiempirical GGA-type density functional constructed with a long-range dispersion correction. J. Comput. Chem. **27**(15), 1787–1799 (2006)

Hu, T., Wang, J., Zhang, H., Li, Z., Hu, M., Wang, X.: Vibrational properties of ti_3c_2 and $ti_3c_2t_2$(t= o, f, oh) monosheets by first-principles calculations: a comparative study. Phys. Chem. Chem. Phys. **17**(15), 9997–10003 (2015)

Hussain, F., Hojjati, M., Okamoto, M., Gorga, R.E.: Review article: polymer-matrix nanocomposites, processing, manufacturing, and application: an overview. J. Compos. Mater. **40**(17), 1511–1575 (2006). https://doi.org/10.1177/0021998306067321

Jafari, A., Tahani, K., Dastan, D., Asgary, S., Shi, Z., Yin, X.-T., Zhou, W.-D., Garmestani, H.: Ştefan Ţălu: Ion implantation of copper oxide thin films; statistical and experimental results. Surf. Interfaces **18**, 100463 (2020)

Katsnelson, M.I., Novoselov, K.S., Geim, A.K.: Chiral tunnelling and the Klein paradox in graphene. Nat. Phys. **2**, 620–625 (2006)

Margine, E.R., Lambert, H., Giustino, F.: Electron-phonon interaction and pairing mechanism in superconducting ca-intercalated bilayer graphene. Sci. Rep. **6**, 21414 (2016)

Naguib, M., Kurtoglu, M., Presser, V., Lu, J., Niu, J., Heon, M., Hultman, L., Gogotsi, Y., Barsoum, M.W.: Two-dimensional nanocrystals produced by exfoliation of ti_3alc_2. Adv. Mater. **23**(37), 4248–4253 (2011). https://doi.org/10.1002/adma.201102306

Naguib, M., Mashtalir, O., Carle, J., Presser, V., Lu, J., Hultman, L., Gogotsi, Y., Barsoum, M.W.: Two-dimensional transition metal carbides. ACS Nano **6**(2), 1322–1331 (2012). https://doi.org/10.1021/nn204153h

Naguib, M., Halim, J., Lu, J., Cook, K.M., Hultman, L., Gogotsi, Y., Barsoum, M.W.: New two-dimensional niobium and vanadium carbides as promising materials for li-ion batteries. J. Am. Chem. Soc. **135**(43), 15966–15969 (2013). https://doi.org/10.1021/ja405735d

Naguib, M., Mashtalir, O., Lukatskaya, M.R., Dyatkin, B., Zhang, C., Presser, V., Gogotsi, Y., Barsoum, M.W.: One-step synthesis of nanocrystalline transition metal oxides on thin sheets of disordered graphitic carbon by oxidation of mxenes. Chem. Commun. **50**, 7420–7423 (2014)

Novoselov, K.S., Geim, A.K., Morozov, S.V., Jiang, D., Zhang, Y., Dubonos, S.V., Grigorieva, I.V., Firsov, A.A.: Electric field effect in atomically thin carbon films. Science **306**(5696), 666–669 (2004). https://doi.org/10.1126/science.1102896

Novoselov, K.S., Mishchenko, A., Carvalho, A., Castro Neto, A.H.: 2d materials and van der Waals heterostructures. Science **353**, 6298 (2016). https://doi.org/10.1126/science.aac9439

Peppas, N., Langer, R.: New challenges in biomaterials. Science **263**(5154), 1715–1720 (1994). https://doi.org/10.1126/science.8134835

Perdew, J.P., Burke, K., Ernzerhof, M.: Generalized gradient approximation made simple. Phys. Rev. Lett. **77**, 3865–3868 (1996)

Pesic, I., Radojevic, V., Barsoum, N. M. Tomic, Romcevic, N.: Preparation, characterization and mechanical properties of mxene/pmma composite. TechConnect World Innovation Conference and Expo, Boston, MA, USA. https://www.techconnectworld.com/World2019/wednesday.htmlW6.26 (2019)

Pešić, J., Gajić, R., Hingerl, K., Belić, M.: Strain-enhanced superconductivity in li-doped graphene. EPL (Europhys. Lett.) **108**(6), 67005 (2014). https://doi.org/10.1209/0295-5075/108/67005

Shan, K., Yi, Z.-Z., Yin, X.-T., Dastan, D., Dadkhah, S., Coates, B.T., Garmestani, H.: Mixed conductivities of a-site deficient Y, Cr-doubly doped srtio3 as novel dense diffusion barrier and temperature-independent limiting current oxygen sensors. Adv. Powder Technol. **31**(12), 4657–4664 (2020)

Shan, K., Yi, Z.-Z., Yin, X.-T., Cui, L., Dastan, D., Garmestani, H., Alamgir, F.M.: Diffusion kinetics mechanism of oxygen ion in dense diffusion barrier limiting current oxygen sensors. J. Alloy. Compd. **855**, 157465 (2021)

Shan, K., Zhai, F., Yi, Z.-Z., Yin, X.-T., Dastan, D., Tajabadi, F., Jafari, A., Abbasi, S.: Mixed conductivity and the conduction mechanism of the orthorhombic CAZRO3 based materials. Surf. Interfaces **23**, 100905 (2021)

Sihvola, A.H.: Electromagnetic Mixing Formulas and Applications, vol. 47. IET, UK (1999)

Tamborra, M., Striccoli, M., Comparelli, R., Curri, M., Petrella, A., Agostiano, A.: Optical properties of hybrid composites based on highly luminescent CDS nanocrystals in polymer. Nanotechnology **15**(4), 240 (2004)

Tan, G.-L., Tang, D., Dastan, D., Jafari, A., Shi, Z., Chu, Q.-Q., Silva, J.P.B., Yin, X.-T.: Structures, morphological control, and antibacterial performance of tungsten oxide thin films. Ceram. Int. **47**(12), 17153–17160 (2021)
Tan, G.-L., Tang, D., Dastan, D., Jafari, A., Silva, J.P.B., Yin, X.-T.: Effect of heat treatment on electrical and surface properties of tungsten oxide thin films grown by HFCVD technique. Mater. Sci. Semicond. Process. **122**, 105506 (2021)
Thomas, K., Sheeba, M., Nampoori, V., Vallabhan, C., Radhakrishnan, P.: Raman spectra of polymethyl methacrylate optical fibres excited by a 532 nm diode pumped solid state laser. J. Opt. A Pure Appl. Opt. **10**(5), 055303 (2008)
Tu, S., Jiang, Q., Zhang, X., Alshareef, H.N.: Large dielectric constant enhancement in mxene percolative polymer composites. ACS Nano **12**(4), 3369–3377 (2018)
Twardowski, T.E.: Introduction to Nanocomposite Materials: Properties, Processing. Characterization, DEStech Publications Inc, Lancaster, USA (2007)
Willis, H., Zichy, V., Hendra, P.: The laser-Raman and infra-red spectra of poly (methyl methacrylate). Polymer **10**, 737–746 (1969)
Zhang, Y., Tan, Y.-W., Stormer, H.L., Kim, P.: Experimental observation of the quantum hall effect and Berry's phase in graphene. Nature **438**, 201–204 (2005)
Zhao, T., Zhang, S., Guo, Y., Wang, Q.: Tic_2: a new two-dimensional sheet beyond mxenes. Nanoscale **8**(1), 233–242 (2016)
Zhu, J., Tang, Y., Yang, C., Wang, F., Cao, M.: Composites of tio2 nanoparticles deposited on ti3c2 mxene nanosheets with enhanced electrochemical performance. J. Electrochem. Soc. **163**(5), 785–791 (2016)